www.ijemr.net ISSN (ONLINE): 2250-0758, ISSN (PRINT): 2394-6962

Volume-7, Issue-4, July-August 2017

International Journal of Engineering and Management Research

Page Number: 27-43

Behaviour of Casson Fluid Slip Flow Past a Vertically Inclined Plate Filled in Porous Medium Submitted in Magnetic Field: Heat Absorption and Chemical Reaction Effects

P. Suresh[1], M. V. Ramana Murthy[2], G.Kamala[3], K. Sreeram Reddy[4]

[1]Department of Mathematics, Chaitanya Bharathi Institute of Technology, Gandipet, Hyderabad, Rangareddy District, Telangana State, INDIA

[2,3,4]Department of Mathematics& Computer Science, University College for Sciences, Osmania University, Hyderabad, Telangana State, INDIA

ABSTRACT

In the present paper, the problem of MHD slip flow of Casson fluid past a vertically inclined plate in a porous medium in presence of chemical reaction, heat absorption and an external magnetic field has been investigated. Heat and mass transfer during Casson fluid flow are also studied. A mathematical model is developed and analyzed by using appropriate mathematical technique, called finite difference method. Expressions for the velocity, temperature, concentration profiles, wall shear stress, rate of heat and mass transfer coefficients have been obtained. The quantitative estimates are presented through graphs and tables. Favourable comparisons with previously published work on various special cases of the problem are obtained.

Keywords-- comparisons, electrically, solutions

Nomenclature:

List of variables:

B_0 Uniform magnetic field (*Tesla*)

A Suction velocity parameter

x' Coordinate axis along the plate (m)

y' Co-ordinate axis normal to the plate (m)

u' Velocity component in $x'-$ direction ($m\ s^{-1}$)

V_o Scale of suction velocity ($m\ s^{-1}$)

T' Fluid Temperature (K)

T'_w Fluid temperature at the wall (K)

T'_∞ Fluid temperature away from the plate (K)

C' Fluid Concentration ($Kg\ m^{-3}$)

C'_w Concentration of the plate ($Kg\ m^{-3}$)

y Dimensionless displacement (m)

C'_∞ Concentration of the fluid far away from the plate ($Kg\ m^{-3}$)

C_p Specific heat at constant pressure $\left(J\ Kg^{-1}K\right)$

Cf The local skin-friction $(N\ m^{-2})$

Nu The local Nusselt number

Sh The local Sherwood number

D Solute mass diffusivity ($m^2\ s^{-1}$)

M Magnetic field parameter

Gr Grashof number for heat transfer

Gc Grashof number for mass transfer

Kr Chemical reaction parameter

u, v Components of velocities along and perpendicular to the plate, respectively ($m\ s^{-1}$)

$\Pr$	Prandtl number
Sc	Schmidt number
Re_x	Reynolds number
g	Acceleration of gravity in magnitude, 9.81 ($m\ s^{-2}$)
t	Time (*sec*)
q_r	Radiative heat flux
p'	Fluid pressure
U_o	Reference velocity ($m\ s^{-1}$)
R	Thermal radiation parameter
Q	Heat absorption parameter
$K_{\lambda w}$	Absorption coefficient
$e_{b\lambda}$	Plank's function
n	Dimensionless exponential index

Greek Symbols:

γ	Casson fluid parameter
ν	Kinematic viscosity ($m^2\ s^{-1}$)
ϕ	Species concentration ($Kg\ m^{-3}$)
ρ	The constant density ($Kg\ m^{-3}$)
β	Volumetric coefficient of thermal expansion (K^{-1})
β^*	Volumetric Coefficient of thermal expansion with concentration ($m^3\ Kg^{-1}$)
σ	Electric conductivity of the fluid $(s\ m^{-1})$
θ	Fluid temperature (K)
ε	Scalar constant $(\varepsilon \le 1)$
λ	Rare fraction parameter
ϕ	Fluid Concentration ($Kg\ m^{-3}$)
α	Angle of inclination of plate ($\deg rees$)
τ'_w	Shear stress $(N\ m^{-2})$
κ	Thermal conductivity of the fluid (W/mK)

Superscripts:

$'$	Dimensionless Properties

Subscripts:

w	Conditions on the wall
∞	Free stream conditions
p	Plate

I. INTRODUCTION

The study of heat and mass transfer with chemical reaction is of considerable importance in chemical and hydrometallurgical industries. The study of heat generation or absorption in moving fluid is important in many problems which are related with chemical reactions and those concerned with dissociating fluids. The possible effects of non-uniform heat generation effects may change the temperature distribution and consequently, the rate of particle deposition in nuclear reactors, semiconductor waters and electronic chips. Chemical reaction can be codified as either heterogeneous or homogeneous processes. Muthucumarswamy and Ganesan [1] as well as Muthucumarswamy [2] studied the first order homogeneous chemical reactions on the flow past an infinite vertical plate. Das et al. [3] considered the effects of a first order chemical reaction on the flow past an impulsively started infinite vertical plate with constant heat flux and mass transfer. Chaudhary and Jha [4] studied on the effect of chemical reactions on MHD micropolar fluid flow past a vertical plate in slip-flow regime. Kandasamy et al. [5] discussed the heat and mass transfer effect along a wedge with a heat source and concentration in the presence of suction/injection taking into account the chemical reaction of the first order. Chemical physiology of flood flow regulation by red cells was discussed by Singel and Stemler [6]. Analytical solutions for heat and mass transfer by laminar flow of a Newtonian, viscous, electrically conducting and heat generating or absorbing fluid on a continuously vertical permeable surface in the presence of a radiation, a first-order homogeneous chemical reaction and the mass flux are reported by Ibrahim et al. [7]. Fairbanks and Wike [8] studied the effects of chemical reaction and diffusion in an isothermal laminar flow along a soluble flat plate. Takhar et al. [9] investigated the flow and mass diffusion of chemical species with first-order and higher order reactions over a continuously stretching sheet with the magnetic field effect. Loganathan et al. [10] investigated the effects of homogeneous first order chemical reaction and mass diffusion on unsteady flow past an impulsively started semi-infinite vertical plate with variable temperature in the presence of thermal radiation. finite difference analysis of MHD convective heat and mass transfer in the presence of first order chemical reaction and thermal

radiation was performed by Sahin Ahmed et al. [11]. Satya Narayana and Sravanthi [12] have analysed the influence of variable permeability on unsteady MHD convection flow past a semi-infinite inclined plate with thermal radiation and chemical reaction. Devika et al. [13] studied the influence of chemical reaction effects on MHD free convection flow in an irregular channel with porous medium. Srinivasa Raju [14] studied transfer effects on an unsteady MHD free convective flow past a vertical plate with chemical reaction using finite element method. Srinivasa Raju et al. [15] found both analytical and numerical solutions of chemically reacting fluid flow induced by an exponentially accelerated infinite vertical plate in a magnetic field and variable temperature via Laplace transform and finite element techniques.

In nature, some non-Newtonian fluids behave like elastic solid that is, no flow occur with small shear stress. Casson fluid is one of such fluids. This fluid has distinct features and is quite famous recently. Casson fluid model was introduced by Casson in 1959 for the prediction of the flow behaviour of pigment-oil suspensions [16]. So, for the flow, the shear stress magnitude of Casson fluid needs to exceed the yield shear stress, otherwise the fluid behaves as a rigid body. This type of fluids can be marked as a purely viscous fluid with high viscosity [17]. Casson model is based on a structure model of the interactive behaviour of solid and liquid phases of a two-phase suspension. Some famous examples of Casson fluid include jelly, tomato sauce, honey, soup and concentrated fruit juices. Human blood can also be treated as Casson fluid due to the presence of several substances such as protein, fibrinogen, globulin in aqueous base plasma and human red blood cells ([18] and [19]). Srinivasa Raju et al. [20] found the numerical solutions of unsteady MHD Casson fluid flow past a vertically inclined surface filled in porous medium in presence of heat flux, viscous dissipation and chemical reaction. Srinivasa Raju [21] found numerical solutions of Casson fluid free convection flow past an infinite vertical plate filled in magnetic field in presence of angle of inclination and thermal radiation. Sailaja et al. [22] studied double diffusive effects on MHD mixed convection casson fluid flow towards a vertically inclined plate filled in porous medium in presence of Biot number. Srinivasa Raju et al. [23] applied finite element technique for finding numerical solutions of MHD casson viscous dissipative fluid flow past a vertically inclined plate in presence of heat and mass transfer.

On the other hand, slip condition has significant applications in various industries and is very efficient in manufacturing process. It is a common belief that heat transfer can be increased by adding velocity slip at the boundary. Beavers and Joseph [24] were the first who used partial slip to the fluid past permeable wall. The addition of velocity slip at wall also plays a vital role for flow in micro devices ([25]). For this reason, researchers have paid considerable attention to include the slip condition at wall rather than no slip condition Nadeem et al. [26] explored the combined effects of partial slip and magnetic field on stagnation point flow of Casson fluid over stretching surface. They concluded that slip parameter reduces the velocity of fluid in the boundary region. Mukhopadhyay [27] studied the effects of slip on viscous fluid over nonlinearly stretching sheet. The problem is solved numerically and it is found that shear stress is an increasing function of slip parameter. The mechanism of slip condition on stagnation point flow of Casson fluid has been reported by Hayat et al. [28]. Hayat et al. ([29] and [30]) investigated the slip effects on boundary layer flow over non-permeable and permeable stretching sheet, respectively. Ahmed and Das [31] studied the effects of thermal radiation and chemical reaction on MHD unsteady mass transfer flow past a semi-infinite vertical porous plate embedded in a porous medium in a slip flow regime with variable suction.

Therefore our work can be considered as extension of Ahmed and Das [31]. The purpose of the present investigation is two-fold. Firstly, it incorporate the effects of magnetic field, chemical reaction, heat absorption by considering the fluid to be electrically conducting. Secondly, the fluid is considered in a porous medium. More exactly, the present work concentres on unsteady MHD free convection flow of a Casson fluid over a vertically inclined plate filled in a porous medium. Numerical solutions are obtained by using the finite difference method. Numerical results for skin-friction, Nusselt and Sherwood numbers are provided. Graphical results are presented and discussed for various physical parameters entering into the problem.

II. MATHEMATICAL FORMULATION

Consider unsteady Casson fluid flow of a incompressible, viscous, electrically conducting and heat absorbing fluid past vertically inclined plate embedded in a uniform porous medium and subjected to a uniform transverse magnetic field in the presence of chemical reaction effects (see Fig. 1). We made the following assumptions.

i. In Cartesian coordinate system, let $x'-$axis is taken to be along the plate and the $y'-$axis normal to the plate. Since the plate is considered infinite in $x'-$direction, hence all physical quantities will be independent of $x'-$direction.

ii. The wall is maintained at constant temperature (T'_w) and concentration (C'_w) higher than the ambient temperature (T'_∞) and concentration (C'_∞) respectively.

iii. It is assumed that there is no applied voltage which implies the absence of an electrical field.

iv. The transversely applied magnetic field and magnetic Reynolds number are assumed to be very small so that the induced magnetic field and the Hall Effect are negligible.

v. The homogeneous chemical reaction is of first order with rate constant $\overline{K}$ between the diffusing species and the fluid is considered.

vi. A consequence of the small magnetic Reynolds number is the uncoupling of the Navier-Stokes equations from Maxwell's equations.

vii. The governing equations for this investigation are based on the balances of mass, linear momentum, energy and concentration species.

viii. The radiative heat flux in the $x'-$direction is considered negligible in comparison to that in $y'-$direction.

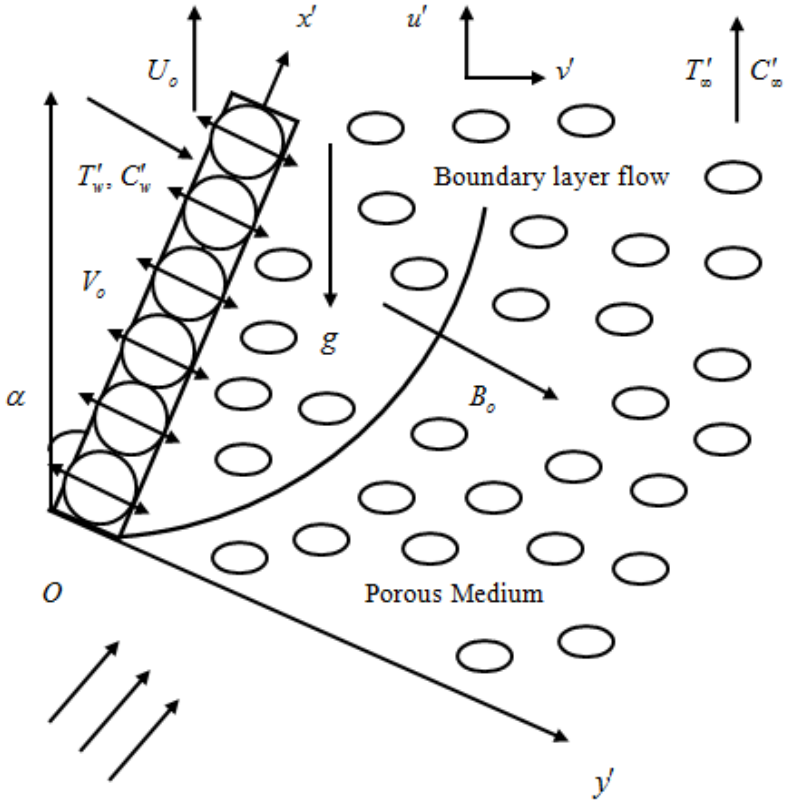

Fig. 1. Geometry of the flow problem

The rheological equation of state for the Cauchy stress tensor of Casson fluid [32] is written as $\tau = \tau_0 + \mu\alpha^*$ (1)

equivalently $\tau_{ij} = \begin{cases} 2\left(\mu_B + \dfrac{p_y}{\sqrt{2\pi}}\right)e_{ij}, & \pi > \pi_c \\ 2\left(\mu_B + \dfrac{p_y}{\sqrt{2\pi_c}}\right)e_{ij}, & \pi < \pi_c \end{cases}$ (2)

where τ is shear stress, τ_0 is Casson yield stress, μ is dynamic viscosity, α^* is shear rate, $\pi = e_{ij}e_{ij}$ and e_{ij} is the $(i,j)^{th}$ component of deformation rate, π is the product based on the non-Newtonian fluid, π_c is a critical value of this product, μ_B is plastic dynamic viscosity of the non-Newtonian fluid,

$$p_y = \frac{\mu_B \sqrt{2\pi}}{\gamma} \tag{3}$$

denote the yield stress of fluid. Some fluids require a gradually increasing shear stress to maintain a constant strain rate and are called Rheopectic, in the case of Casson fluid (Non-Newtonian) flow where $\pi > \pi_c$

$$\mu = \mu_B + \frac{p_y}{\sqrt{2\pi}} \tag{4}$$

Substituting Eq. (3) into Eq. (4), then, the kinematic viscosity can be written as

$$\nu = \frac{\mu}{\rho} = \frac{\mu_B}{\rho}\left(1 + \frac{1}{\gamma}\right) \tag{5}$$

Taking into consideration the assumptions made above, these equations can be written in Cartesian frame of reference, as follows:

Continuity Equation:

$$\frac{\partial v'}{\partial y'} = 0 \tag{6}$$

Momentum Equation:

$$\frac{\partial u'}{\partial t'} + v'\frac{\partial u'}{\partial y'} = -\frac{1}{\rho}\left(\frac{\partial p'}{\partial x'}\right) + \nu\left(1 + \frac{1}{\gamma}\right)\frac{\partial^2 u'}{\partial y'^2} - \left[\frac{\sigma B_o^2}{\rho}\right]u' - \left[\frac{\nu}{K'}\right]u' + g\beta\left(T' - T'_\infty\right)(\cos\alpha) + g\beta^*\left(C' - C'_\infty\right)(\cos\alpha) \tag{7}$$

Energy Equation:

$$\frac{\partial T'}{\partial t'} + v'\frac{\partial T'}{\partial y'} = \frac{\kappa}{\rho C_p}\frac{\partial^2 T'}{\partial y'^2} - \frac{1}{\rho C_p}\left[Q_o\left(T' - T'_\infty\right)\right] - \frac{1}{\rho C_p}\left(\frac{\partial q_r}{\partial y'}\right) \tag{8}$$

Concentration Equation:

$$\frac{\partial C'}{\partial t'} + v'\frac{\partial C'}{\partial y'} = D\frac{\partial^2 C'}{\partial y'^2} - k'_r\left(C' - C'_\infty\right) \tag{9}$$

Under these assumptions, the appropriate boundary conditions for the velocity, temperature and concentration fields are

$$\left.\begin{array}{l} t' \le 0 : u' = 0,\ T' = T'_\infty,\ C' = C'_\infty \quad for\ \ all\ \ y' \\ t' > 0 : \begin{cases} u' = h'\left(\dfrac{\partial u'}{\partial y'}\right),\ T' = T'_w + \varepsilon\left(T'_w - T'_\infty\right)e^{n't'},\ C' = C'_w + \varepsilon\left(C'_w - C'_\infty\right)e^{n't'} \ \ at\ \ y' = 0 \\ u' \to U'_\infty = U_o\left(1 + \varepsilon e^{n't'}\right),\ T' \to T'_\infty,\ C' \to C'_\infty \ \ as\ \ y' \to \infty \end{cases} \end{array}\right\} \tag{10}$$

From equation (6), it is clear that the suction velocity at the plate is a function of time only. Assuming that it takes the following exponential form:

$$v' = -V_o\left(1 + \varepsilon A e^{n't'}\right) \tag{11}$$

Where A is a real positive constant, ε is a positive constant and εA is small values less than unity, and V_o is scale of suction velocity which is non-zero positive constant. The negative sign indicates that the suction is towards the plate. Outside the boundary layer, equation (7) gives

$$-\frac{1}{\rho}\left(\frac{\partial p'}{\partial x'}\right) = \frac{dU'_\infty}{dt'} + \left[\frac{\nu}{k'}\right]U'_\infty + \frac{\sigma}{\rho}B_o^2 U'_\infty \tag{12}$$

As mentioned earlier, in the case of optically thin limit, the fluid cannot absorb its own emitted radiation, but it absorbs the radiation emitted by boundaries. Following Cogley et al. [33], the rate of flux of radiation in the optically thin limit for a non-gray gas near equilibrium is given by

$$\frac{\partial q_r}{\partial y} = 4I\left(T' - T'_\infty\right) \tag{13}$$

Where $I = \int_0^\infty K_{\lambda w}\left(\frac{de_{b\lambda}}{dT'}\right)d\lambda$.

In order to write the governing equations and the boundary conditions in dimensionless from, the following non-dimensional quantities are introduced.

$$\left.\begin{aligned} &y = \frac{y'V_o}{\nu},\ t = \frac{t'V_o^2}{\nu},\ u = \frac{u'}{U_o},\ v = \frac{v'}{V_o},\ \theta = \frac{T'-T'_\infty}{T'_w - T'_\infty},\ \phi = \frac{C'-C'_\infty}{C'_w - C'_\infty},\ n = \frac{n'\nu}{V_o^2},\ U_p = \frac{u'_p}{U_o},\\ &M = \left(\frac{\sigma B_o^2}{\rho}\right)\frac{\nu}{V_o^2},\ Gr = \frac{g\beta\nu\left(T'_w - T'_\infty\right)}{U_o V_o^2},\ Gc = \frac{g\beta^*\nu\left(C'_w - C'_\infty\right)}{U_o V_o^2},\ \Pr = \frac{\nu\rho C_p}{\kappa},\ Sc = \frac{\nu}{D},\\ &K = \frac{K'V_o^2}{\nu^2},\ R = \frac{4\nu I}{\rho C_p V_o^2},\ U_\infty = \frac{U'_\infty}{U_o},\ h = \frac{h'V_o}{\nu},\ Kr = \frac{k'_r\nu}{V_o^2},\ Q = \frac{Q_o\nu}{\rho C_p V_o^2} \end{aligned}\right\} \tag{14}$$

In view of equations (6), (7) and (8), equations (2) to (4) reduce to the following dimensional form:

$$\frac{\partial u}{\partial t} - \left(1 + \varepsilon A e^{nt}\right)\frac{\partial u}{\partial y} = \frac{dU_\infty}{dt} + \left(1 + \frac{1}{\gamma}\right)\frac{\partial^2 u}{\partial y^2} + (Gr)(\cos\alpha)\theta + (Gc)(\cos\alpha)\phi + \left(M + \frac{1}{K}\right)(U_\infty - u) \tag{15}$$

$$\frac{\partial \theta}{\partial t} - \left(1 + \varepsilon A e^{nt}\right)\frac{\partial \theta}{\partial y} = \frac{1}{\Pr}\frac{\partial^2 \theta}{\partial y^2} - Q\theta - R\theta \tag{16}$$

$$\frac{\partial \phi}{\partial t} - \left(1 + \varepsilon A e^{nt}\right)\frac{\partial \phi}{\partial y} = \frac{1}{Sc}\frac{\partial^2 \phi}{\partial y^2} - Kr\phi \tag{17}$$

The corresponding initial and boundary conditions in dimensionless form are:

$$\left.\begin{aligned} &t \le 0:\ u = 0,\ \theta = 0,\ \phi = 0 \quad for \quad all \quad y\\ &t > 0:\begin{cases} u = \lambda\left(\frac{\partial u}{\partial y}\right),\ \theta = 1 + \varepsilon e^{nt},\ \phi = 1 + \varepsilon e^{nt} \quad at \quad y = 0\\ u \to U_\infty = 1 + \varepsilon e^{nt},\quad \theta \to 0,\quad \phi \to 0 \quad as \quad y \to \infty \end{cases} \end{aligned}\right\} \tag{18}$$

All the physical parameters are defined in the nomenclature. It is now important to calculate the physical quantities of primary interest, which are the local wall shear stress, the local surface heat and mass flux. The velocity, temperature and concentration fields in the boundary layer, we can now calculate the local wall shear stress (i.e., skin-friction), Rate of heat and mass transfer in dimensionless form are given by

Skin-friction: Knowing the velocity field, the skin-friction at the plate can be obtained, which in non-dimensional form is given by

$$C_f = \frac{\tau'_w}{\rho U_o V_o}\left(1 + \frac{1}{\gamma}\right) = \left(1 + \frac{1}{\gamma}\right)\left[\frac{\partial u}{\partial y}\right]_{y=0} \tag{19}$$

Rate of heat transfer (Nusselt number): Knowing the temperature field, the heat transfer coefficient can be obtained which in the non-dimensional form, in terms of the Nusselt number, is given by

$$Nu = \left[\frac{x'}{(T'_w - T'_\infty)}\frac{\partial T'}{\partial y'}\right]_{y'=0} \Rightarrow Nu\left(\mathrm{Re}_x^{-1}\right) = \left[\frac{\partial \theta}{\partial y}\right]_{y=0} \tag{20}$$

Rate of mass transfer (Sherwood number): Knowing the concentration filed, the rate of mass transfer coefficient can be obtained, which in the non-dimensional form, in terms of the Sherwood number, is given by

$$Sh = \left[\frac{x'}{(C'_w - C'_\infty)}\frac{\partial C'}{\partial y'}\right]_{y'=0} \Rightarrow Sh\left(\mathrm{Re}_x^{-1}\right) = \left[\frac{\partial \phi}{\partial y}\right]_{y=0} \quad (21)$$

Where $\mathrm{Re}_x = -\dfrac{V_o x'}{\nu}$ is the Reynold's number.

III. NUMERICAL SOLUTIONS BY FINITE DIFFERENCE METHOD

The non-linear momentum and energy equations given in equations (15), (16) and (17) are solved under the appropriate initial and boundary conditions (18) by the implicit finite difference method. The transport equations (15), (16) and (17) at the grid point (i, j) are expressed in difference form using Taylor's expansion. The momentum, energy and concentration equations reads.

$$\left(\frac{u_i^{j+1}-u_i^j}{\Delta t}\right)-\frac{B}{2}\left(\frac{u_{i+1}^{j+1}-u_{i-1}^{j+1}}{\Delta y}+\frac{u_{i+1}^{j}-u_{i-1}^{j}}{\Delta y}\right)=\left(n\varepsilon e^{nt}\right)+\left(1+\frac{1}{\gamma}\right)\left(\frac{u_{i-1}^{j+1}-2u_i^{j+1}+u_{i+1}^{j+1}}{2(\Delta y)^2}+\frac{u_{i-1}^{j}-2u_i^{j}+u_{i+1}^{j}}{2(\Delta y)^2}\right)$$
$$+(Gr)\left(\frac{\theta_i^{j+1}+\theta_i^j}{2}\right)(\cos\alpha)+(Gc)\left(\frac{\phi_i^{j+1}+\phi_i^j}{2}\right)(\cos\alpha)+N\left(1+\varepsilon e^{nt}\right)-N\left(\frac{u_i^{j+1}+u_i^j}{2}\right) \quad (16)$$

$$\left(\frac{\theta_i^{j+1}-\theta_i^j}{\Delta t}\right)-\frac{B}{2}\left(\frac{\theta_{i+1}^{j+1}-\theta_{i-1}^{j+1}}{\Delta y}+\frac{\theta_{i+1}^{j}-\theta_{i-1}^{j}}{\Delta y}\right)=\frac{1}{\mathrm{Pr}}\left(\frac{\theta_{i-1}^{j+1}-2\theta_i^{j+1}+\theta_{i+1}^{j+1}}{2(\Delta y)^2}+\frac{\theta_{i-1}^{j}-2\theta_i^{j}+\theta_{i+1}^{j}}{2(\Delta y)^2}\right)$$
$$-(Q+R)\left(\frac{\theta_i^{j+1}+\theta_i^j}{2}\right) \quad (17)$$

$$\left(\frac{\phi_i^{j+1}-\phi_i^j}{\Delta t}\right)-\frac{B}{2}\left(\frac{\phi_{i+1}^{j+1}-\phi_{i-1}^{j+1}}{\Delta y}+\frac{\phi_{i+1}^{j}-\phi_{i-1}^{j}}{\Delta y}\right)=\frac{1}{Sc}\left(\frac{\phi_{i-1}^{j+1}-2\phi_i^{j+1}+\phi_{i+1}^{j+1}}{2(\Delta y)^2}+\frac{\phi_{i-1}^{j}-2\phi_i^{j}+\phi_{i+1}^{j}}{2(\Delta y)^2}\right)$$
$$-Kr\left(\frac{\phi_i^{j+1}+\phi_i^j}{2}\right) \quad (18)$$

Where $B = 1+\varepsilon A e^{nt}$ and $N = M + \dfrac{1}{K}$. Corresponding boundary and initial conditions are:

$$\left.\begin{aligned} &u_{i,0}=0,\ \theta_{i,0}=0,\ \phi_{i,0}=0 \quad for\ \ all\ \ i \\ &u_{0,j}=\lambda\left(\frac{u_1^j-u_0^j}{\Delta y}\right),\ \theta_{0,j}=1+\varepsilon e^{njt},\ \phi_{0,j}=1+\varepsilon e^{njt} \\ &u_{X,j}\to U_\infty=1+\varepsilon e^{njt},\ \ \theta_{X,j}\to 0,\ \ \phi_{X,j}\to 0 \end{aligned}\right\} \quad (19)$$

Thus the values of u, θ and ϕ at grid point $t = 0$ are known; hence the temperature and concentration profiles have been solved at time $t_{i+1} = t_i + \Delta t$ using the known values of the previous time $t = t_i$ for all $i = 1, 2, ..., N-1$. Then the velocity field is evaluated using the already known values of temperature and concentration profiles obtained at $t_{i+1} = t_i + \Delta t$. These processes are repeated till the required solution of u, θ and ϕ is gained at convergence criteria.

$$abs\left|(u,\ \theta,\ \phi)_{exact}-(u,\ \theta,\ \phi)_{numerical}\right| < 10^{-3} \quad (29)$$

IV. VALIDATION OF CODE

Table-1: Comparison of present skin-friction (*Cf*) results with the skin-friction (*Cf* *) results of Ahmed and Das [31].

Sc	*M*	*Kr*	*K*	*Q*	*λ*	*Gr*	*Gc*	*Cf*	*Cf* *
0.60	3.0	1.0	1.0	1.0	0.3	6.0	4.0	3.1899206481	3.194506
0.78								2.9801334921	2.9820064
	5.0							2.6531448287	2.679543
		2.0						0.5503996218	0.5904764
			10.5					3.4520075184	3.4687398
				10.5				2.2513004877	2.2527005
					0.6			2.7623448106	2.772427
						4.0		2.7036689557	2.7236035
							2.0	2.9731447055	2.9747134

Table-2: Comparison of present Nusselt number (*Nu*) results with the Nusselt number (*Nu) results of Ahmed and Das [31].**

Q	*Nu*	*Nu**
0.50	2.4806648713	2.4960342
1.00	2.3363180466	2.3589459
10.5	2.1934480699	2.2108416

Table-3: Comparison of present Sherwood number (*Sh*) results with the Sherwood number (*Sh) results of Ahmed and Das [31].**

Sc	*Kr*	*Sh*	*Sh**
0.60	1.0	1.3875543059	1.394154
0.78		1.2635574098	1.270695
	2.0	0.7496652864	0.755311

In order to ascertain the accuracy of the present numerical results, the present finite difference method results are compared with the previous analytical results of Ahmed and Das [31] for $\gamma \to \infty$ and $\alpha = 0^o$ in tables 1, 2 and 3. They are found to be in an excellent agreement.

V. RESULTS AND DISCUSSIONS

The problem of MHD free convective Casson fluid flow past a vertically inclined plate in presence of slip, chemical reaction and heat absorption effects is addressed in this study. Numerical calculations have been carried out for the non-dimensional velocity, temperature and concentration profiles, keeping the other parameters of the problem fixed. Numerical calculations of these results are presented graphically in Figs. 2-18. These results show the effect of material parameters such as Magnetic parameter *M*, Permeability parameter *K*, Grashof number for heat transfer *Gr*, Grashof number for mass transfer *Gc*, Prandtl number Pr, Schmidt number *Sc*, Casson fluid parameter *γ*, Angle of inclination parameter *α*, Heat absorption parameter *Q*, Thermal radiation parameter *R*, Chemical reaction parameter *Kr*, Rare fraction parameter (Slip parameter) *λ* and time *t* on velocity, temperature and concentration profiles. Also the results of skin-friction coefficient due to velocity, rate of heat transfer coefficient (Nusselt number) due to temperature and mass transfer coefficient (Sherwood number) due to concentration are presented in tabular form. To find out the solution of this problem, we have placed an infinite vertical plate in a finite length in the flow. Hence, we solve the entire problem in a finite boundary. However, in the graphs, the *y* values vary from 0 to 9 and the velocity, temperature and concentration profiles tend to zero as *y* tends to 9. This is

true for any value of *y*. Thus, we have considered finite length.

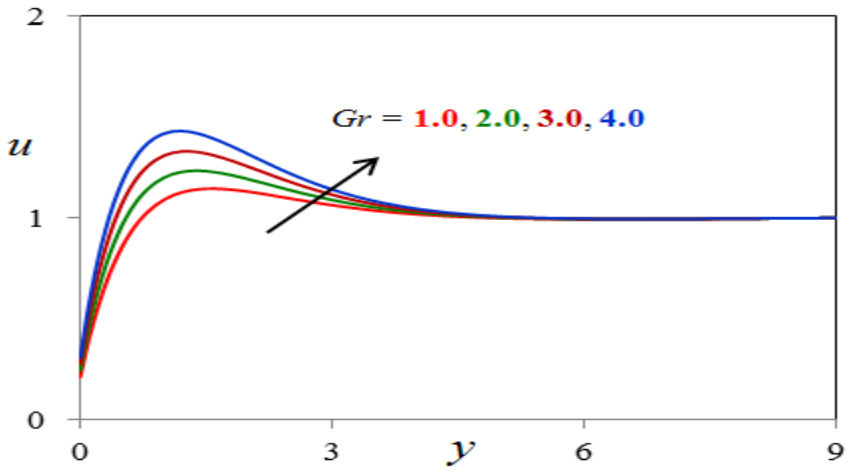

Fig. 2. *Gr* effect on velocity profiles

Figs. 2 and 3 exhibit the effect of Grashof number for heat transfer *Gr* and Grashof number for mass transfer *Gc* on the velocity profile with other parameters are fixed. The Grashof number for heat transfer *Gr* signifies the relative effect of the thermal buoyancy force to the viscous hydrodynamic force in the boundary layer. As expected, it is observed that there is a rise in the velocity due to the enhancement of thermal buoyancy force. Also, as *Gr* increases, the peak values of the velocity increases rapidly near the porous plate and then decays smoothly to the free stream velocity. The Grashof number for mass transfer *Gc* defines the ratio of the species buoyancy force to the viscous hydrodynamic force. As expected, the fluid velocity increases and the peak value is more distinctive due to increase in the species buoyancy force. The velocity distribution attains a distinctive maximum value in the vicinity of the plate and then decreases properly to approach the free stream value. It is noticed that the velocity increases with increasing values of the Grashof number for mass transfer *Gc*. The effect of the Magnetic field parameter *M* is shown in Fig. 4. It is observed that the velocity of the fluid decreases with the increase of the magnetic field number values. The decrease in the velocity as the Magnetic field parameter *M* increases is because the presence of a magnetic field in an electrically conducting fluid introduces a force called the Lorentz force, which acts against the flow if the magnetic field is applied in the normal direction, as in the present study. This resistive force slows down the fluid velocity component as shown in Fig. 4. Fig. 5 shows the effect of the permeability parameter (porous medium) *K* on the velocity distribution. As shown, the velocity is increasing with the increasing *K*. Physically, this result can be achieved when the holes of the porous medium may be neglected.

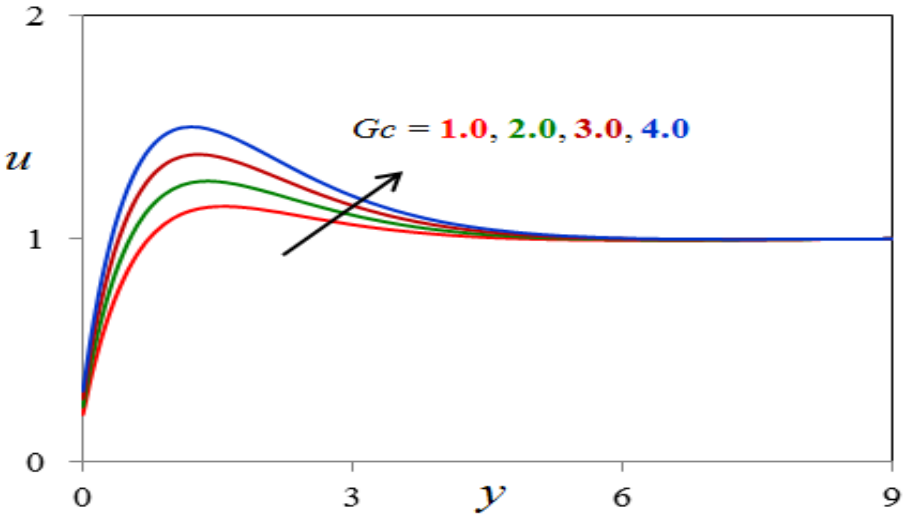

Fig. 3. *Gc* effect on velocity profiles

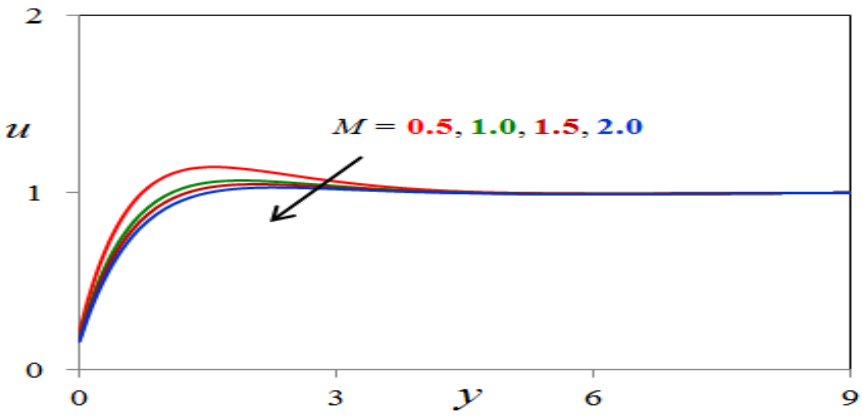

Fig. 4. *M* effect on velocity profiles

The velocity profiles in the Fig. 6 shows that rate of motion is significantly reduced with increasing of Casson fluid parameter γ. Also, it is observed from this Fig. 6, the boundary layer momentum thickness decreases as increase of Casson fluid parameter γ. The effect of angle of inclination of the plate α on the velocity field has been illustrated in Fig. 7. It is seen that as the angle of inclination of the plate α increases the velocity field decreases. Fig. 8 illustrates the effect of thermal radiation parameter R on the velocity profiles. It is seen from this figure that there is a steady decrease in the velocity with the increase in radiation parameter R. The increase in this parameter R leads to increase the boundary layer thickness and to reduce the heat transfer rate in the presence of thermal buoyancy force. The effect of thermal radiation parameter R on temperature profiles against y is displayed in Fig. 9. It is observed from Fig. 9 that the temperature profiles decreases as the thermal radiation parameter R increases. This result qualitatively agrees with expectation, since the effect of radiation is to decrease the rate of energy transport to the fluid, thereby decreasing the temperature of the fluid.

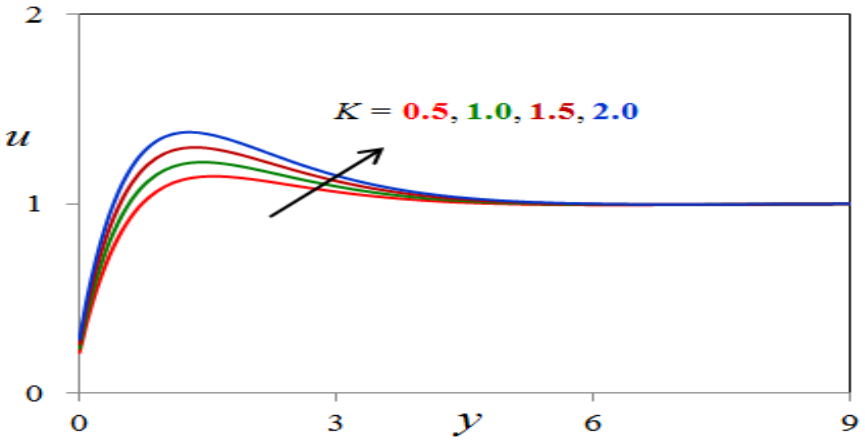

Fig. 5. *K* effect on velocity profiles

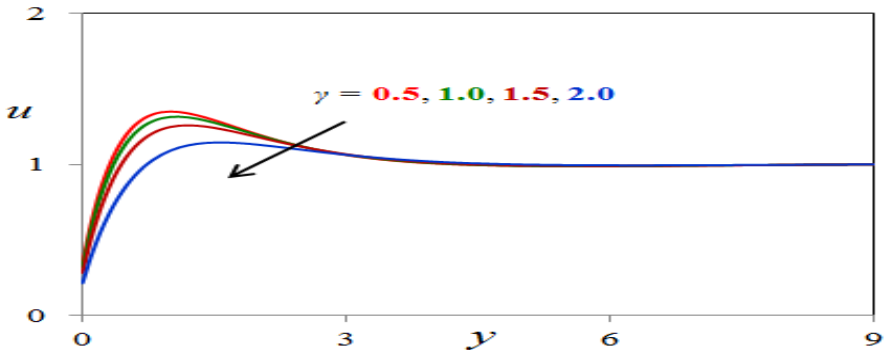

Fig. 6. γ effect on velocity profiles

Figs. 10 and 11 illustrate the influence of Heat absorption parameter Q on the velocity and temperature at t = 1.0 respectively. Physically speaking, the presence of heat absorption (thermal sink) effects has the tendency to reduce the fluid temperature. This causes the thermal buoyancy effects to decrease resulting in a net reduction in the fluid velocity. These behaviours are clearly obvious from Figs. 10 and 11. Figs. 12 and 13 display the effects of the chemical reaction parameter Kr on the velocity and concentration profiles, respectively. As expected, the presence of the chemical reaction significantly affects the concentration profiles as well as the velocity profiles. It should be mentioned that the studied case is for a destructive chemical reaction Kr. In fact, as chemical reaction Kr increases, the considerable reduction in the velocity profiles is predicted, and the presence of the peak indicates that the maximum value of the velocity occurs in the body of the fluid close to the surface but not at the surface. Also, with an increase in the chemical reaction parameter, the concentration decreases. It is evident that the increase in the chemical reaction Kr significantly alters the concentration boundary layer thickness but does not alter the momentum boundary layers.

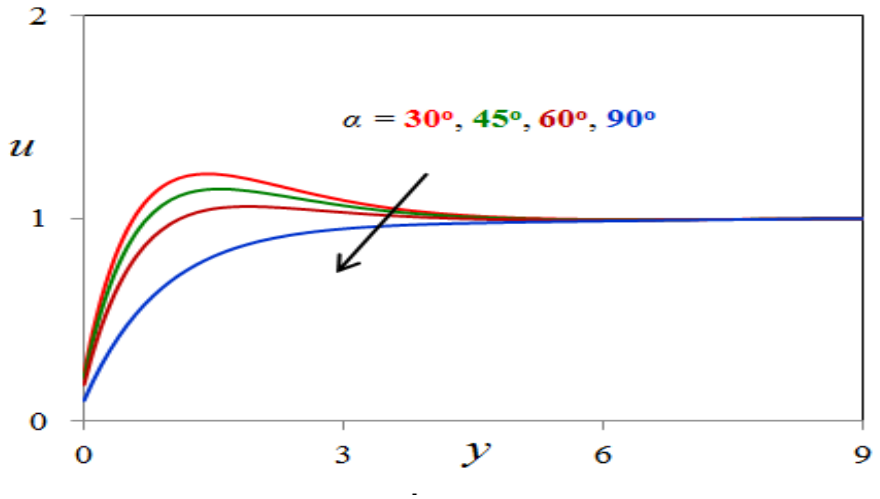

Fig. 7. α effect on velocity profiles

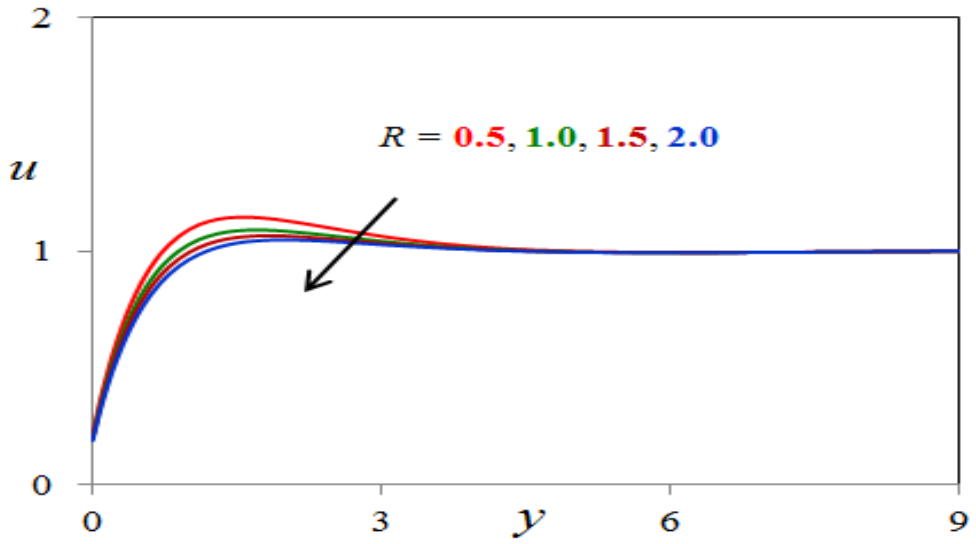

Fig. 8. R effect on velocity profiles

In Fig. 14 we depict the effect of Prandtl number Pr on the temperature field. It is observed that an increase in the Prandtl number leads to decrease in the temperature field. Also, temperature field falls more rapidly for water in comparison to air and the temperature curve is exactly linear for mercury, which is more sensible towards change in temperature. From this observation it is conclude that mercury is most effective for maintaining temperature differences and can be used efficiently in the laboratory. Air can replace mercury, the effectiveness of maintaining temperature changes are much less than mercury. However, air can be better and

cheap replacement for industrial purpose. This is because, either increase of kinematic viscosity or decrease of thermal conductivity leads to increase in the value of Prandtl number Pr. Hence temperature decreases with increasing of Prandtl number Pr. Fig. 15 shows the concentration field due to variation in Schmidt number *Sc* for the gasses Hydrogen (*Sc* = 0.22), Helium (*Sc* = 0.30), Water-vapour (*Sc* = 0.60), Oxygen (*Sc* = 0.66) and Ammonia (*Sc* = 0.78). It is observed that concentration field is steadily for Hydrogen and falls rapidly for Oxygen and Ammonia in comparison to Water-vapour. Thus Hydrogen can be used for maintaining effective concentration field and Water-vapour can be used for maintaining normal concentration field. Fig. 16 displays that the velocity profiles increases as rarefaction parameter λ are increased indicating the fact that slips at the surface accelerates the fluid motion. Figs. 17 and 18 display the effect of time *t* on both temperature and concentration profiles against *y*. From these two figures, we observed that both the temperature and concentration profiles are increasing with increase of time *t*.

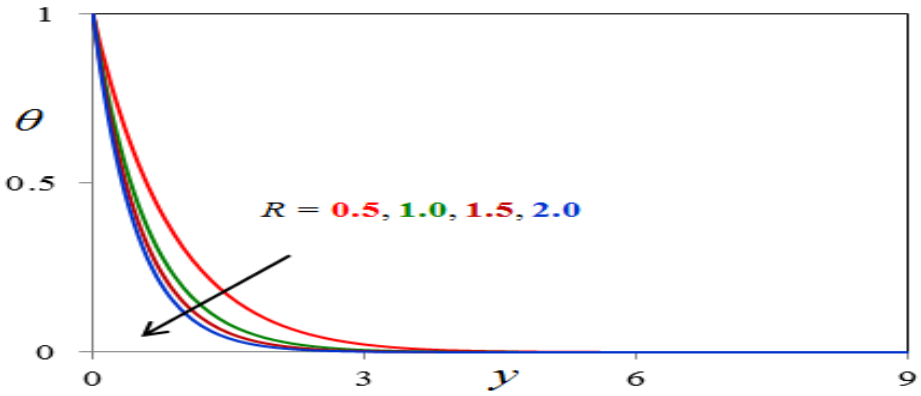

Fig. 9. *R* effect on temperature profiles

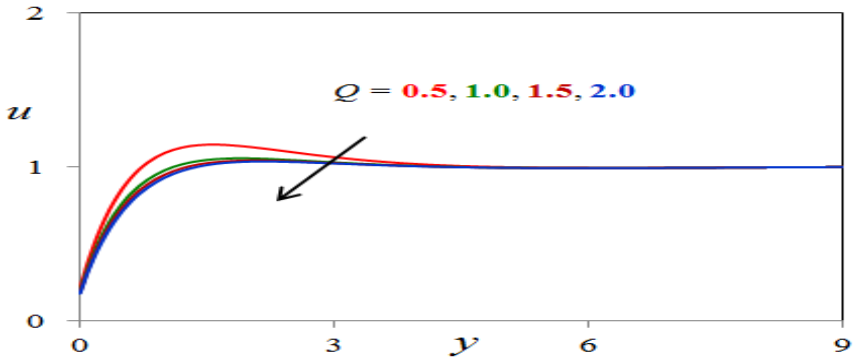

Fig. 10. *Q* effect on velocity profiles

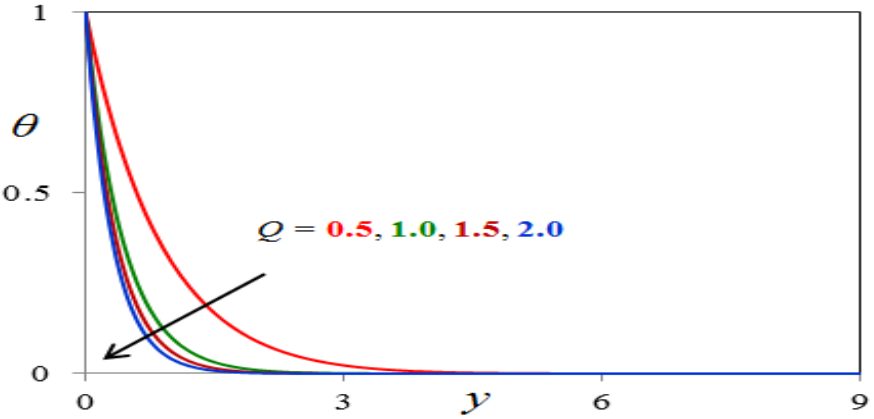

Fig. 11. Q effect on temperature profiles

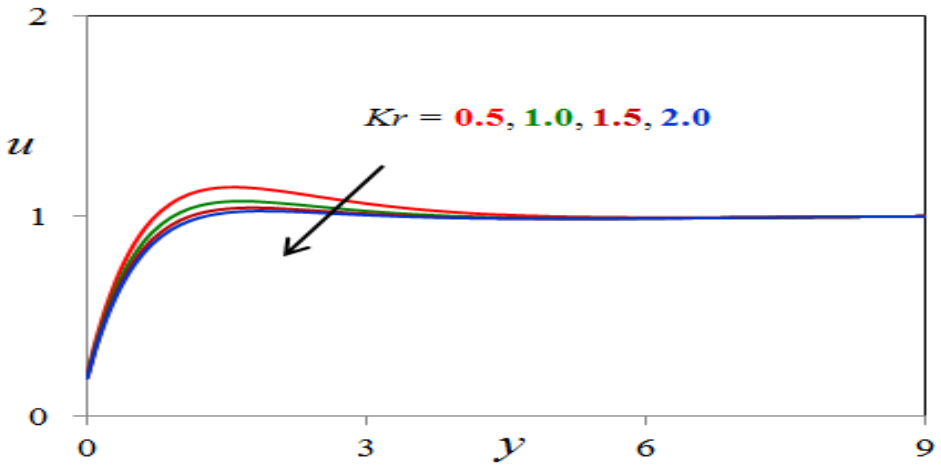

Fig. 12. *Kr* effect on velocity profiles

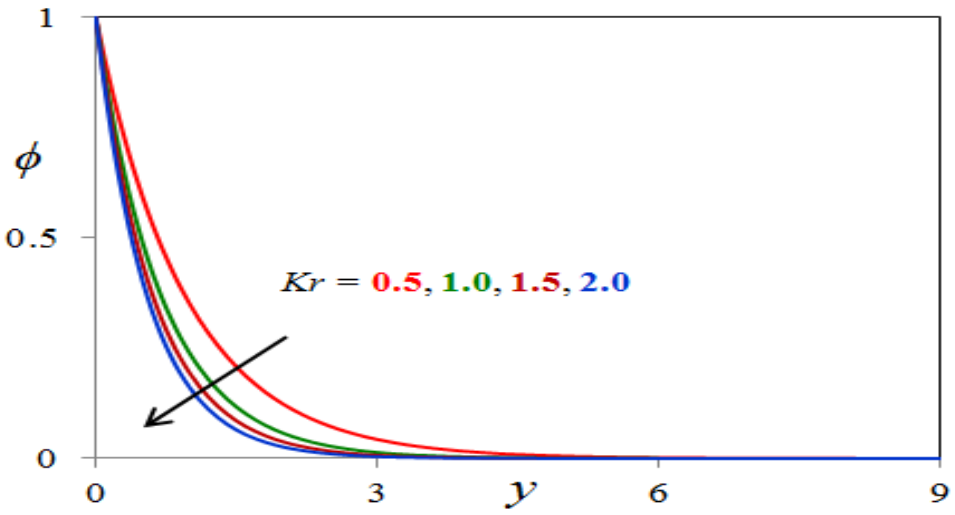

Fig. 13. *Kr* effect on concentration profiles

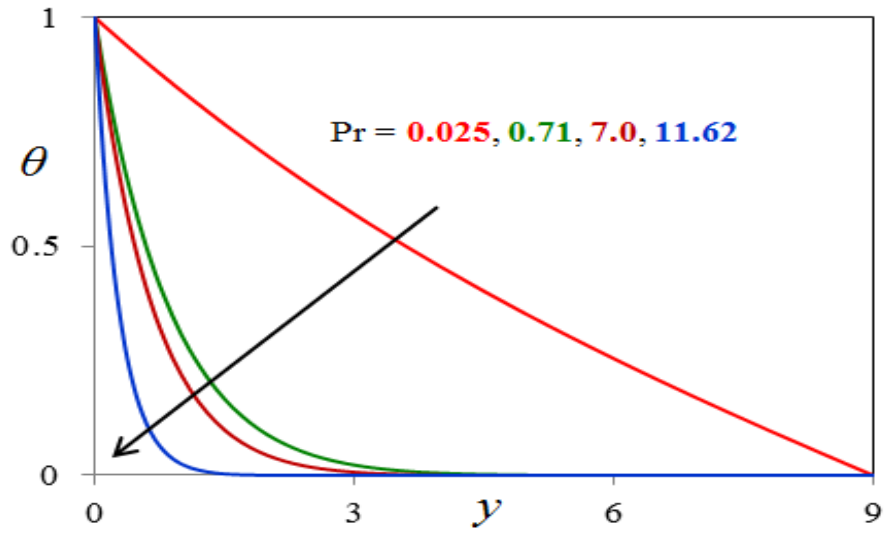

Fig.14. Pr effect on temperature profiles

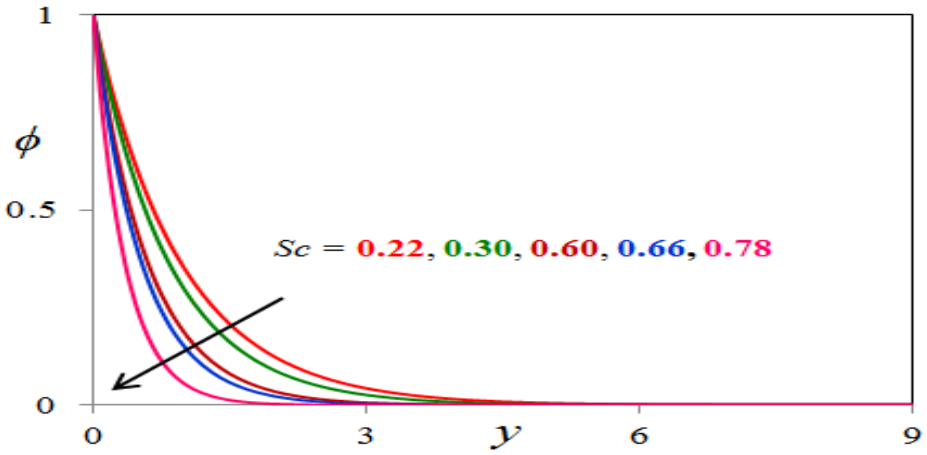

Fig. 15. *Sc* effect on concentration profiles

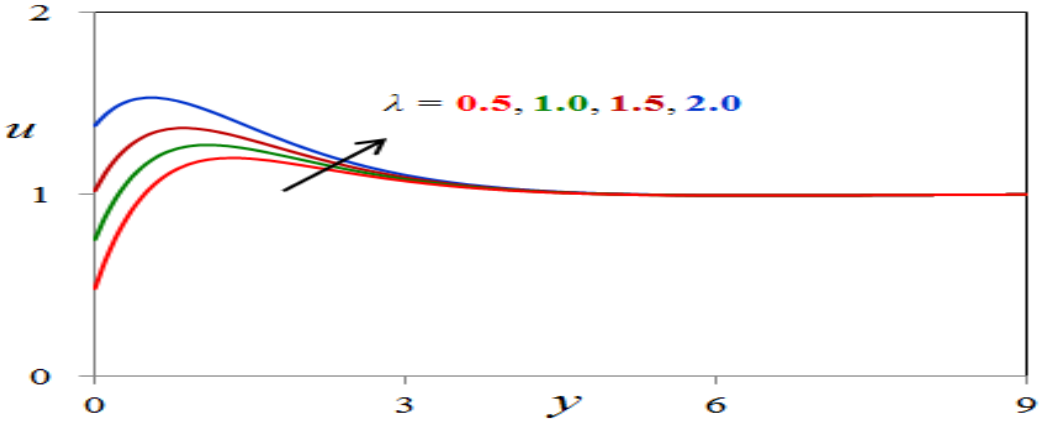

Fig. 16. λ effect on velocity profiles

The profiles for skin-friction coefficient due to velocity profiles under the effects Magnetic parameter *M*, Permeability parameter *K*, Grashof number for heat transfer *Gr*, Grashof number for mass transfer *Gc*, Prandtl number Pr, Schmidt number *Sc*, Casson fluid parameter γ, Angle of inclination parameter α, Heat absorption parameter *Q*, Thermal radiation parameter *R*, Chemical reaction parameter *Kr*, Rare fraction parameter (Slip parameter) λ and time *t* are presented in the table-4. From this table, we observed that, the skin-friction coefficient rises under the effects of Permeability parameter *K*, Grashof number for heat transfer *Gr*, Grashof number for mass transfer *Gc*, Rare fraction parameter (Slip parameter) λ and time *t* and falls under the effects of Magnetic parameter *M*, Prandtl number Pr, Schmidt number *Sc*, Casson fluid parameter γ, Angle of inclination parameter α, Heat absorption parameter *Q*, Thermal radiation parameter *R* and Chemical reaction parameter *Kr*.

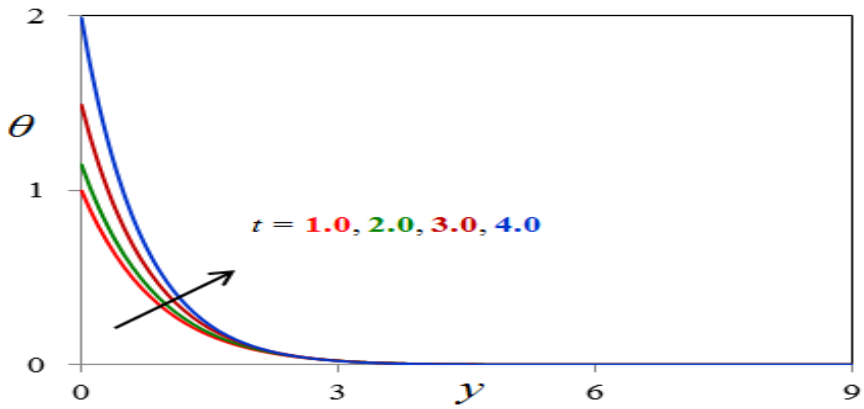

Fig. 17. *t* effect on temperature profiles

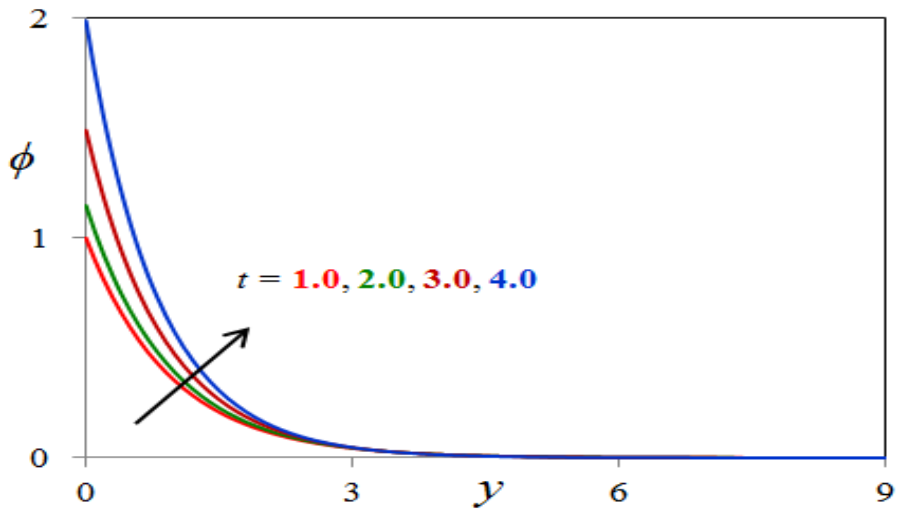

Fig. 18. *t* effect on concentration profiles

The profiles for rate of heat transfer coefficient (Nusselt number) due to temperature profiles under the effects of Prandtl number Pr, Heat absorption parameter *Q*, Thermal radiation parameter *R* and time *t* is presented in table-5. We see from this table, the Nusselt number falls under the effects of Prandtl number Pr, Heat absorption parameter *Q*, Thermal radiation parameter *R* and rises under the effect of time *t*. The profiles for rate of mass transfer coefficient (Sherwood number) due to concentration profiles under the effect of Schmidt number *Sc* and Chemical reaction parameter *Kr* and time *t* are presented in the table-6. From this table, we observed that, the Sherwood number decreases under the effects of Schmidt number *Sc*, Chemical reaction parameter *Kr* and increases under the effect of time *t*.

Table-4: Skin-friction coefficient results

Gr	*Gc*	*M*	*K*	Pr	*Sc*	*Q*	*R*	*Kr*	λ	γ	α	*t*	*Cf*
2.0	2.0	0.5	0.5	0.71	0.22	0.5	0.5	0.5	0.5	0.5	30^o	1.0	2.982247681839
4.0	2.0	0.5	0.5	0.71	0.22	0.5	0.5	0.5	0.5	0.5	30^o	1.0	3.156682473318
2.0	4.0	0.5	0.5	0.71	0.22	0.5	0.5	0.5	0.5	0.5	30^o	1.0	3.204412786347
2.0	2.0	1.0	0.5	0.71	0.22	0.5	0.5	0.5	0.5	0.5	30^o	1.0	2.871301525640
2.0	2.0	0.5	1.0	0.71	0.22	0.5	0.5	0.5	0.5	0.5	30^o	1.0	3.104215666841
2.0	2.0	0.5	0.5	7.00	0.22	0.5	0.5	0.5	0.5	0.5	30^o	1.0	2.943271183032
2.0	2.0	0.5	0.5	0.71	0.30	0.5	0.5	0.5	0.5	0.5	30^o	1.0	2.962331945072
2.0	2.0	0.5	0.5	0.71	0.22	1.0	0.5	0.5	0.5	0.5	30^o	1.0	2.973004812475
2.0	2.0	0.5	0.5	0.71	0.22	0.5	1.0	0.5	0.5	0.5	30^o	1.0	2.985541178015
2.0	2.0	0.5	0.5	0.71	0.22	0.5	0.5	1.0	0.5	0.5	30^o	1.0	2.971200586334
2.0	2.0	0.5	0.5	0.71	0.22	0.5	0.5	0.5	1.0	0.5	30^o	1.0	3.046018533913
2.0	2.0	0.5	0.5	0.71	0.22	0.5	0.5	0.5	0.5	1.0	30^o	1.0	2.950483376618
2.0	2.0	0.5	0.5	0.71	0.22	0.5	0.5	0.5	0.5	0.5	45^o	1.0	2.941088731669
2.0	2.0	0.5	0.5	0.71	0.22	0.5	0.5	0.5	0.5	0.5	30^o	2.0	3.124339017781

Table-5: Rate of heat transfer coefficient (Nusselt number) results

Pr	*R*	*Q*	*t*	*Nu*
0.71	0.5	0.5	1.0	2.153048617699
7.00	0.5	0.5	1.0	1.995144702841

0.71	1.0	0.5	1.0	2.051175569982
0.71	0.5	1.0	1.0	2.063992247833
0.71	0.5	0.5	2.0	2.210566074424

Table-6: Rate of mass transfer coefficient (Sherwood number) results

Sc	*Kr*	*t*	*Sh*
0.22	0.5	1.0	1.102445834492
0.30	0.5	1.0	0.926447339281
0.22	1.0	1.0	0.996117461830
0.22	0.5	2.0	1.216924483069

VI. CONCLUSIONS

In this study, we have found the numerical solutions of coupled partial differential governing equations for unsteady hydromagnetic free convection Casson fluid slip flow past a vertically inclined porous plate in the presence of thermal radiation, chemical reaction and heat absorption. Employing finite difference method, the leading equations are solved numerically. The present results to illustrate the flow characteristics for the velocity, temperature and concentration profiles as well as the skin-friction, Nusselt number and Sherwood number show how the flow fields are influenced by the material parameters of the flow problem. Our investigation of the problem setup leads to the following conclusions:

1. It is observed that the velocity of the fluid increases with the increasing of parameters *K*, *Gr*, *Gc*, λ, *t* and decreases with the increasing of parameters *M*, Pr, *Sc*, γ, α, *Q*, *R*, *Kr*.
2. The fluid temperature increases with the increasing of *t* and decreases with the increasing of Pr, *Q* and *R*.
3. The Concentration of the fluid decreases with the increasing of *Sc*, *Kr* and increases with increasing of *t*.
4. The shear stress at the wall rises under the effects of *K*, *Gr*, *Gc*, λ, *t* and falls under the effects of *M*, Pr, *Sc*, γ, α, *Q*, *R*, *Kr*.
5. The heat flux or rate of heat transfer coefficient from the plate to the fluid is reduced under the influences of Pr, *Q* and *R*.
6. The mass flux or rate of mass transfer coefficient from the plate to the fluid is reduced under the influence of *Sc* and *Kr*.
7. Both the heat and mass fluxes are increasing with increasing values of *t*.
8. On comparing present numerical results with the analytical results of Ahmed and Das [31], it can be seen that they agree very well.

REFERENCES

[1] R. Muthucumarswamy, P. Ganesan, First order chemical reaction on flow past an impulsively started vertical plate with uniform heat and mass flux, Acta Mech., 147 (2001), pp. 45-57.

[2] R. Muthucumarswamy, Effects of a chemical reaction on moving isothermal vertical surface with suction, Acta Mech., 155 (2002), pp. 5-70.

[3] U.N. Das, R.K. Deka, V.M. Soundalgekar, Effects of mass transfer on flow past an impulsively started infinite vertical plate with constant heat flux and chemical reaction, Forsch. Ingenieurwesen (Eng. Res.), 60 (1994), pp. 284-287.

[4] R. C. Chaudhary, P. Jain, Effects of chemical reactions on MHD micropolar fluid flow past a vertical plate in slip-flow regime, Appl. Math. Mech., 29 (2000), pp. 1179-1194.

[5] R. Kandasamy, K. Periasamy, K. K. P. Sivagnana, Effects of chemical reaction, heat and mass transfer along wedge with heat source and concentration in the presence of suction or injection, Int. J. Heat Mass Transfer, 48 (2005), pp. 388-1394.

[6] D. J. Singel, J. S. Stemler, Chemical physiology of flood flow regulation by red cells: the role of nitric oxide and S-Nitrosohemoglobin, Annu. Rev. Physiol., 67 (2005), pp. 99-145.

[7] F. S. Ibrahim, A. M. Elaiw, A.A. Bakr, Effect of the chemical reaction and radiation absorption on the unsteady MHD free convection flow past a semi infinite vertical permeable moving plate with heat source and suction, Commun. Nonlinear Sci. Numer. Simul., 13 (2008), pp. 1056-1066.

[8] D. F. Fairbanks, C. R. Wike, Diffusion and chemical reaction in and isothermal laminar flow along a soluble flat plate, Ind. Eng. Chem. Res., 42 (1950), pp. 471-475.

[9] H. S. Takhar, A. J. Chamkha, G. Nath, Flow and mass transfer on a stretching sheet with magnetic field and chemically reactive species, Int. J. Eng. Sci., 38 (2000), pp. 1303-1314.

[10] P. Loganathan, T. Kulandaivel, R. Muthucumaraswamy, First order chemical reaction on moving semi-infinite vertical plate in the presence of optically thin gray gas, Int. J. Appl. Math. Mech., 4 (2008), pp. 26-41.

[11] Sahin Ahmed, Joaquin Zueco, L. M. Lopez-Ochoa, Numerical modelling of MHD convective heat and mass transfer in presence of first order chemical reaction and thermal radiation, Chem. Eng. Commun., 201 (2013), pp. 419-436.

[12] P. V. Satya Narayana, S. Sravanthi, Influence of variable permeability on unsteady MHD convection flow past a semi-infinite inclined plate with thermal radiation and chemical reaction, J Energy Heat Mass Transfer, 34 (2012), pp. 143-161.
[13] B. Devika, P. V. Satya Narayana, S. Venkataramana, Chemical reaction effects on MHD free convection flow in an irregular channel with porous medium, Int J Math Arch, 4 (4) (2013), pp. 282-295.
[14] R. Srinivasa Raju, Transfer Effects On An Unsteady MHD Free Convective Flow Past A Vertical Plate With Chemical Reaction, *Engineering Transactions Journal*, pp. 1 - 29, 2017.
[15] R. Srinivasa Raju, G. Aruna, N. V. Swamy Naidu, S. Vijay Kumar Varma, M. M. Rashidi, Chemically reacting fluid flow induced by an exponentially accelerated infinite vertical plate in a magnetic field and variable temperature via LTT and FEM, *Theoretical Applied Mechanics*, Vol. 43, Issue 1, pp. 49 - 83, 2016.
[16] N. Casson, A flow equation for the pigment oil suspensions of the printing ink type, Rheology of Disperse Systems, Pergamon, New York (1959), pp. 84-102.
[17] K. Bhattacharyya, T. Hayat, A. Alsaedi, Exact solution for boundary layer flow of Casson fluid over a permeable stretching/shrinking sheet, Z. Angew. Math. Mech., 10 (2013), pp. 1-7.
[18] R. K. Dash, K. N. Mehta, G. Jayaraman, Casson fluid flow in a pipe filled with a homogeneous porous medium, Int. J. Eng. Sci., 34 (1996), pp. 1145-1156,
[19] Y. C. Fung, Biodynamics circulation, Springer-Verlag, New York (1984).
[20] R. Srinivasa Raju, B. Mahesh Reddy, G. Jithender Reddy, Influence Of Angle Of Inclination On Unsteady MHD Casson Fluid Flow Past A Vertical Surface Filled By Porous Medium In Presence Of Constant Heat Flux, Chemical Reaction And Viscous Dissipation, *Journal of Nanofluids*, Vol. 6, pp. 668 - 679, 2017.
[21] R. Srinivasa Raju, Numerical Treatment Of Casson Fluid Free Convection Flow Past An Infinite Vertical Plate Filled In Magnetic Field In Presence Of Angle Of Inclination And Thermal Radiation: A Finite Element Technique, International Journal of Engineering and Applied Sciences, Vol. 8, No. 4, pp. 119 - 133, 2016.
[22] S. V. Sailaja, B. Shanker, R. Srinivasa Raju, Double Diffusive Effects On MHD Mixed Convection Casson Fluid Flow Towards A Vertically Inclined Plate Filled In Porous Medium In Presence Of Biot Number: A Finite Element Technique, Journal of Nanofluids, Vol. 6, pp. 420 - 435, 2017, https://doi.org/10.1166/jon.2017.1337.
[23] R. Srinivasa Raju, G. Jithender Reddy and G. Anitha, MHD Casson Viscous Dissipative Fluid Flow Past A Vertically Inclined Plate In Presence Of Heat And Mass Transfer: A Finite Element Technique, Frontiers In Heat And Mass Transfer, Vol. 8, pp. 27, 2017.
[24] G. S. Beavers, D.D. Joseph, Boundary conditions at a naturally permeable wall, J. Fluid Mech., 30 (1967), pp. 197-207.
[25] M. Gad-el-hak, The fluid mechanics of microdevices-the freeman scholar lecture, J. Fluids Eng., 121 (1999), pp. 5-33.
[26] S. Nadeem, R. Mehmood, N. S. Akbar, Combined effects of magnetic field and partial slip on obliquely striking rheological fluid over a stretching surface, J. Magn. Magn. Mater., 378 (2015), pp. 457-462.
[27] S. Mukhopadhyay, Analysis of boundary layer flow over a porous nonlinearly stretching sheet with partial slip at the boundary, Alexandria Eng. J., 52 (2013), pp. 563-569.
[28] T. Hayat, M. Farooq, A. Alsaedi, Thermally stratified stagnation point flow of Casson fluid with slip conditions, Int. J. Numer. Methods Heat Fluid Flow, 25 (2015), pp. 724-748.
[29] T. Hayat, T. Javed, Z. Abbas, Slip flow and heat transfer of a second grade fluid past a stretching sheet through a porous space, Int. J. Heat Mass Transf., 51 (2008), pp. 4528-4534.
[30] T. Hayat, M. Qasim, S. Mesloub, MHD flow and heat transfer over permeable stretching sheet with slip conditions, Int J. Numer. Methods Fluids, 66 (2011), pp. 963-975.
[31] N. Ahmed, K. K. Das, MHD Mass Transfer Flow past a Vertical Porous Plate Embedded in a Porous Medium in a Slip Flow Regime with Thermal Radiation and Chemical Reaction, Open Journal of Fluid Dynamics, 2013, 3, 230-239, http://dx.doi.org/10.4236/ojfd.2013.33028.
[32] Dash, R. K., Mehta, K. N., Jayaraman, G.: Casson Fluid Flow in a Pipe Filled with a Homogeneous Porous Medium. Int. J. Eng. Sci. 34, 1145-1156 (1996).
[33] Cogley, A. C., Vincentine, W. C., and Gilles, S. E., 1968, Differential Approximation for Radiative Transfer in a Non-Gray Gas Near Equilibrium," AIAA J., Vol. 6, pp. 551-555.